Journal of Engineering Physics and Thermophysics, Vol. 74, No. 6, 2001

USE OF CERAMIC COATINGS AS THERMAL BARRIERS IN HEAT CYCLING

N. M. Chigrinova

UDC 691.9.048.4

Within the context of a phenomenological model of the process of anode microarc oxidation (AMO) some features of the formation of ceramic coatings have been investigated. Experimental results are reported which confirm the good coincidence of the calculated and experimental data on the creation, by the AMO method, of effective layers with the required properties and a prescribed microstructure. With the example of the pistons of highly augmented internal combustion engines, the efficiency is shown of using the developed composition of an electrolyte and the proposed range of electrophysical parameters of the AMO technology for creation of thermal barriers on the critical surfaces of complex configuration of thermostressed units functioning under conditions of heat cycling.

In a number of modern production processes associated with the operation of units and mechanisms under extreme conditions, in particular, under conditions of heat-cyclic loads, the problem of thermal protection of the working surfaces of products against thermal overloads acquires fundamental importance. As the versions of thermal protection, it is proposed to use different inserts made of materials with a low thermal conductivity, coolant loops, and ceramic spacers resistant to thermal actions [1, 2]. However, the use of the mentioned heat-shielding materials involves problems or is impossible in thermostressed units whose working surfaces are of complex configuration.

As an efficient means of thermal protection of thermostressed units of any structural shape and function, use can be made of thermal ceramic barriers which are grown directly on the working surface and follow its configuration [3]. Such layers represent, as a rule, a combination of a coating and a diffusion layer with a transformed structure in the surface regions of a product, have 100% adhesion to a substrate, and possess high cyclic heat resistance and resistance to high-temperature corrosive wear [4].

Recently, to form thermal barriers use has been made of electrochemical methods, in particular, anodic oxidation, which is conventionally subdivided into four groups [5]: thick-layer, spark, microarc, and arc.

A characteristic form of the dependence of the voltage on the duration of the process of anodic oxidation for all the groups mentioned (the so-called "coating-forming curves") is shown in Fig. 1.

In all the cases, portion I on the graph corresponds to the stage of formation of a thin anodic film; the fundamental principles of the theory of its growth have been developed by Vervy and Mott [6]. The dependence of the ionic current (I_i) forming the film on the field intensity (E) with fixed initial and final conditions is represented as

$$I_i = A \exp BE \,. \tag{1}$$

According to the Faraday law that relates the quantity I_i to the rate of change of the thickness of an anodic oxide film (dh/dt), the constants A and B can be expressed as [6]

Scientific-Research Institute of Powder Metallurgy with Pilot Production, Minsk, Belarus. Translated from Inzhenerno-Fizicheskii Zhurnal, Vol. 74, No. 6, pp. 167–173, November–December, 2001. Original article submitted December 26, 2000.

1062-0125/01/7406-1583$25.00

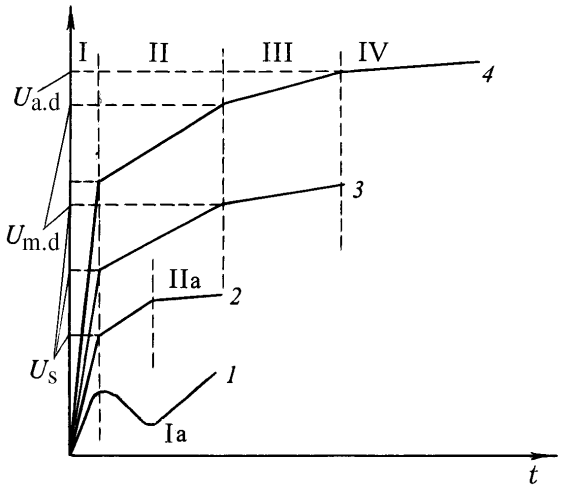

Fig. 1. Coating-forming curves in the processes of anodic oxidation: 1) thick-layer; 2) spark; 3) microarc; 4) arc. *U*, V; *t*, min.

$$dh/dt = NV\nu \exp(-W_1 + W_2 - qa_bE)/kT\,, \tag{2}$$

where V is the volume of the oxide film per ion, on the average (the ion is potentially capable of moving); W_1 is the difference of the potential energies of the ions on the top of the barrier in the initial state; W_2 is the contribution to the effective activation energy which takes integral account of the fact that ions in both the initial and transient (intermediate) positions are in the complicated "dynamic" state rather than in the "static" state.

Portions II on curves 2 and 3 correspond to the sparking stage. It is known that such a stage can also occur in the processes of thick-layer anodic oxidation following Fig. 1a; however, as is asserted in [7], it is highly improbable to reach useful sparking and especially microarc oxidation without changing the electrolyte composition.

On curve 2, three portions with a different rate of increase of the voltage can be noted. In interval I from the beginning of the process to the sparking voltage (U_s), two types of empirical dependences of the residual current on the voltage are established [8, 9]. For small values of the final voltage U_f^* these dependences turned out to be exponential:

$$I = a \exp bU \tag{3}$$

with empirical constants a and b regularly related to both the conditions of the process of formation of a coating and the moment of its interruption. For $U_f^* > 100$ V, the general form of the relation between U and I, which is adequate to the experiment, becomes somewhat different:

$$I = a_1 U^{b_1}\,, \quad b_1 > 1\,. \tag{4}$$

In interval II from the sparking voltage to the so-called maximum voltage (U_{max}), sparks do not prevent the growth of the coating but retard it. And, finally, in interval IIa, above the maximum voltage, sparks prevent the coating growth. A significant visual difference in spark discharges to the maximum voltage and above it has also been noted. Guntershulze and Betz called the former sparks metallic since the quantity U_s substantially depended on the nature of the metal, while the latter sparks were termed electrolytic ones since U_{max} depended almost exclusively on the nature of the electrolyte [10]. The electrolyte influences U_s as well, but the anionic component of the solution rather than pH turns out to be decisive. Thus, the phenomenological foundation of theoretical concepts of sparking processes has been laid.

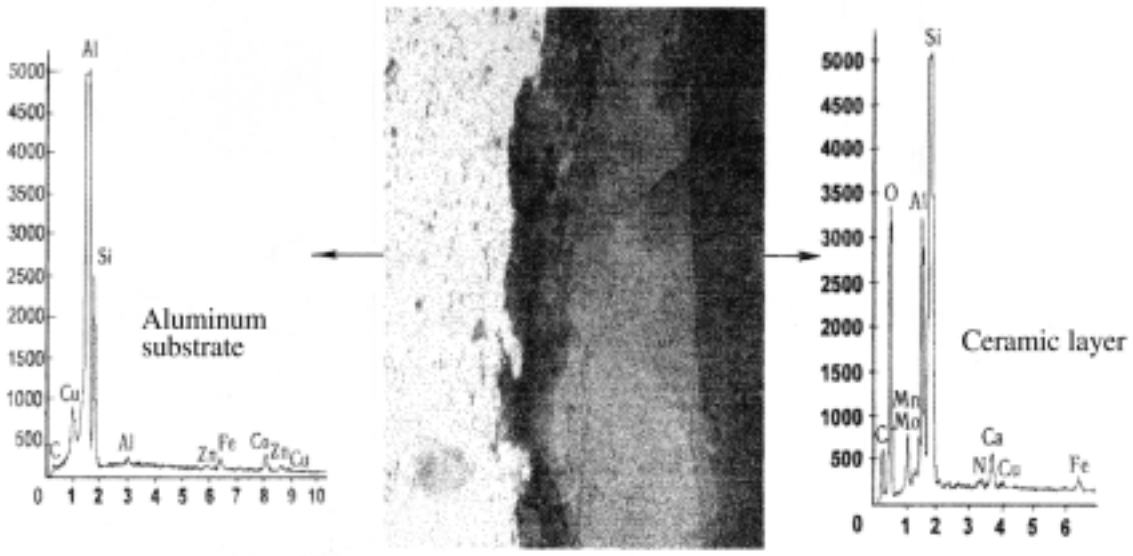

Fig. 2. Structure and phase composition of a ceramic AMO coating (the vertical, line intensity, pulses; the horizontal, position of the line 2θ, deg).

From the viewpoint of the quality of the protective layers formed the most useful is the stage of microarc discharges, since, owing to the high temperature occurring in plasma discharges on the metal surface in an electrolyte, it is precisely in this stage that the fusion of oxide residues proceeds [11].

Proceeding from the foregoing, the method of anodic microarc oxidation is the most acceptable for the formation of thermal barriers on the critical surfaces of products of complex configuration.

A distinctive feature of the AMO technology is the formation of ceramic oxide coatings on the surface of products; there coatings are formed in weakly alkaline solutions of the electrolyte under the action of electric microarc discharges on the material. In this case, a coating based on the most thermodynamically stable oxide of the basic material with a low concentration of spinel compounds and oxides of the elements entering into the electrolyte composition is formed in the product treated (Fig. 2) [12].

The basis for the research [13–15] and technological [16, 17] developments of the AMO method is the phenomenological fact of a regular change of the stages of a technological process which are characterized by certain sets of discharges and combinations of the related physical and chemical processes. Such an approach is employed in the currently available phenomenological model of an anodic microarc process which is based on the analysis and description of its stages [12, 13].

According to [5, 18], to evaluate the parameters of the process of microarc oxidation one conventionally relates the change of the stages to the abscissas of the points of intersection t_i of their rectified segments on the curve $U(t)$ (Fig. 3), which allows determination of the duration of the stages ($t_i - t_{i-1}$), the initial voltages (U_s, $U_{m.d}$), and the mean rates of growth (with respect to the slope of the tan β_1, tan β_2, and tan β_3). The total density of the current at any instant (t) can be represented with the same degree of conditionality by three components, namely, discharge-free ($j_{1(t)}$), spark ($j_{2(t)}$), and microarc ($j_{3(t)}$) modes of charge transfer, respectively:

$$j = j_{1(t)} + j_{2(t)} + j_{3(t)} = \alpha_{1(t)} j + \alpha_{2(t)} j + \alpha_{3(t)} j \,. \tag{5}$$

The oxidized surface can also be subdivided into three components:

$$S = S_{1(t)} + S_{2(t)} + S_{3(t)} = S_{1(t)} + N^*_{2(t)}\, S^*_{2(t)} + N^*_{3(t)}\, S^*_{3(t)} \,. \tag{6}$$

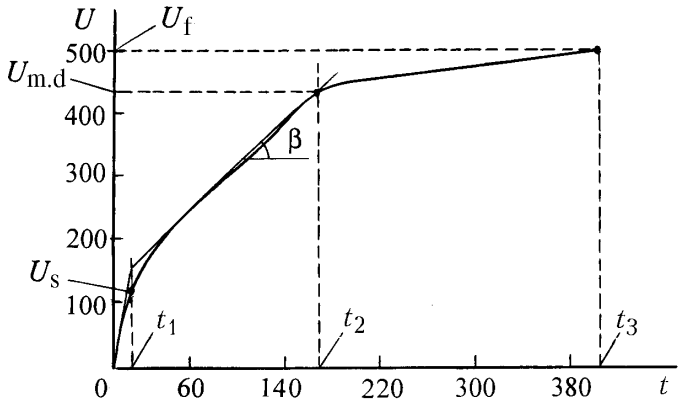

Fig. 3. Coating-forming curve of the anodic microarc process on the deformed alloy in the phosphate electrolyte. *U*, V; *t*, min

From Eqs. (5) and (6) it follows that

$$j_{2(t)} = N^*_{2(t)} j^*_{2(t)} S^*_{2(t)} / S \,, \tag{7}$$

$$j_{3(t)} = N^*_{3(t)} j^*_{3(t)} S^*_{3(t)} / S \,. \tag{8}$$

The derivative $dU/d\tau$ can be represented in the form

$$(dU/d\tau)_{...t} = (dU/dh)_{...t} (dh/dm)_{...t} (dm/d\tau)_{...t} \,, \tag{9}$$

In this case

$$(dh/dm)_{...t} = 1/S\rho_{...t} \tag{10}$$

or

$$(dh/dm)_{...t} = jS\eta_{...t} \,. \tag{11}$$

From Eqs. (9), (10), and (11) we obtain the following expression for interpretation of the curves:

$$(dU/d\tau)_{...t} = j\eta_{...t} / [\rho_{...t} (dU/dh)_{...t}] \,. \tag{12}$$

For a partial description of the transition regions and some refinement of the model using the data of Guntershulze and Betz [10] for coatings with specific characteristics acquired by a certain instant of their formation (t), one can use the general regularity

$$U - U_e = a^*_{i(t)} j^{b^*_{i(t)}} \,. \tag{13}$$

With account for Eq. (13) and information on the characteristic shape of the curves $U(t)$ for the first stage we take the following model:

$$U_{(t)} - U_{e(t)} = a_1 h_{(t)} j_1^{b_1} \,. \tag{14}$$

With the given initial conditions the first spark discharges appear only from a certain potential U_s^0 ($U_s^0 \le U_s$). Here, in the spark and microarc stages, the number of discharges, i.e., j_2 or j_3, increases with the

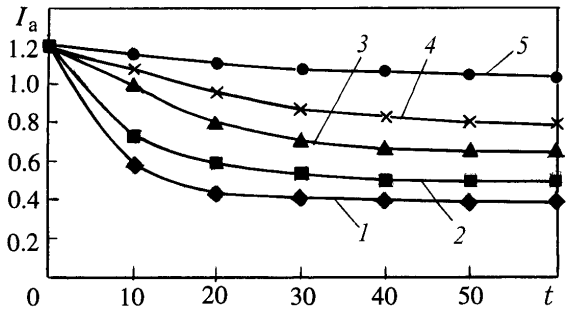

Fig. 4. Anodic current versus time of the AMO process in different compositions of the electrolyte. I_a, A; t, min.

current density but $U(t)$ almost does not change. Taking into account the general character of the curves and of the dependence $h = \varphi(t)$, we can assume that, for instance, in the sparking stage (at least locally in a certain vicinity of t) the relation

$$U_{(t)} - U_s^0 - U_{e(t)} = a_{2(t)}\, h_{(t)}\, j_2^{b_{2(t)}} \tag{15}$$

holds, where $b_{2(t)}$ is a parameter which is very close to zero and $U_{(t)} \geq U_s^0$. It is possible that a fixed pair of the parameters a_2 and b_2 will turn out to be sufficient to describe the entire stage. For the transition region, from (14) and (15) we obtain

$$U_s^0 / h_{(t)} = a_1\, j_{1(t)}^{b_1} - a_2\, j_{2(t)}^{b_2}\,, \tag{16}$$

assuming, as an approximation, that the values of $U_{e(t)}$ in two current channels acting in parallel are the same (i.e., depend only on the line current).

We can easily extend these ideas to the second transition region by adding a combination of the conjugate empirical parameters $U_{m.d}^0$, a_3, and b_3 to them. As a whole, the constructed mathematical model (5)–(16) satisfactorily corresponds to the totality of data available in the literature [18–27].

To sum up, we can draw the conclusion that two factors, namely, the chemical composition of the electrolyte and the electrophysical parameters of the process, exert a decisive influence on the character and distinctive features of formation of effective ceramic coatings by the AMO method.

The above calculations of the electrophysical parameters have been obtained as applied to the standard composition of an electrolyte based on liquid glass. However in the indicated solution, in which the final potential (U_f) is achieved and microarc discharges do not appear on the oxidized surface, friable oxide layers with a thickness of several microns and a metastable structure can be formed. Such ceramic layers cannot provide efficient thermal protection in thermostressed structures.

Therefore, for implementation of thermal protection of thermostressed units and mechanisms operated under conditions of heat cycling by the AMO method an attempt has been made to develop the optimum composition of the electrolyte in which a barrier of effective thickness with the required heat resistance and heat stability can be formed.

The electrolyte efficiency evaluated by the consumed electric energy in obtaining a functional AMO coating and determined by its chemical activity is also manifested as a decrease in the power intensity of the AMO process and reduction in the time of formation of ceramic layers of effective thicknesses.

Comparison of the kinetic features of the process of formation of a ceramic coating in electrolytes of different composition has shown that in the electrolyte of composition 1 (a solution of 2.5–7.5 g/liter of liquid glass) (Fig. 4) it is impossible to obtain an AMO coating with a thickness of more than 5 μm. In the electrolyte of composition 2 based on liquid glass with addition of sodium hydroxide (0.3–0.4 g/liter), a wear-

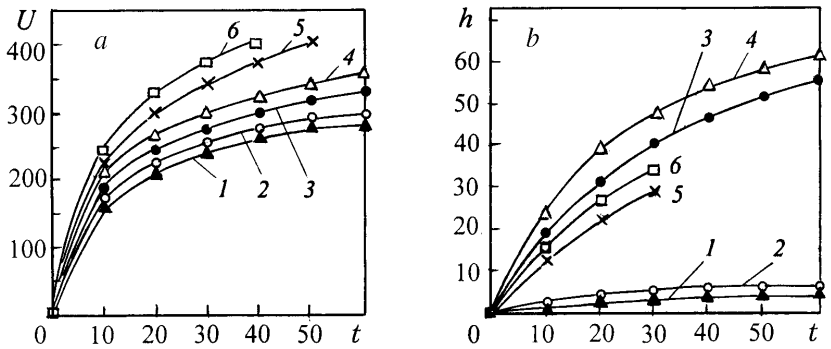

Fig. 5. Change in the voltage of formation (a) and in the thickness (b) of the coating versus time in the galvanostatic regime for different current densities: 1) j = 1, 2) 2, 3) 3, 4) 4, 5) 5, and 6) 6 A/dm^2. U, V; h, μm; t, min.

resistant coating of the required quality is formed. However, it is seen from Fig. 4 that in conducting the AMO process in the indicated composition of the electrolyte, the anodic current virtually becomes stabilized at the 20th minute and the surface oxide layer ceases to grow. This is indicative of the impossibility of obtaining in composition 2 a coating with a thickness of more than 20 μm.

The formation of a ceramic coating in an electrolyte containing 1 g/liter of potassium hydroxide (KOH) and 6 g/liter of sodium silicate (Na_2SiO_3) (composition 3) proceeded more intensely and allowed us to obtain a layer of effective thickness; however, this took no less than 2 h, which makes this version uneconomical. Microstructural studies have revealed a drawback of the ceramic coating formed for its use as a protective barrier. The two-layer coating formed, whose internal layer represents a very thin monolithic fused film, has an external porous layer with numerous inclusions of phases of mullite, i.e., a chemical compound possessing extremely low strength, adhesion, and heat resistance, which does not allow its use as a reliable thermal protection.

One of the efficient electrolytes composed of sodium hydroxide in an amount of 2.5 g/liter, sodium aluminate in an amount of 3 g/liter, and sodium hexametaphosphate in an amount of 3 g/liter (composition 4) provides the formation of a coating with a thickness of up to 70 μm with an optimum microstructure. However, it has been noted that with further growth of the oxide layer a loose unstable mullite phase is formed on the edges of the sample.

The combination of the enumerated chemical ingredients in one electrolyte often promotes the accelerated precipitation of salts from the solution, which makes the coatings nonuniform in thickness.

For the purpose of optimizing the chemical composition of an electrolyte that ensures the formation of ceramic layers capable of acting as thermal barriers on the critical surfaces of thermostressed structures, the electrolyte based on sodium hydroxide, sodium aluminate, and sodium hexametaphosphate has been modified by achieving a certain ratio between the basic components and the additives of the known chemical elements and compounds (composition 5) developed at the Scientific-Research Institute of Powder Metallurgy (Minsk, Belarus). The characteristics of a ceramic coating obtained in this electrolyte and its microstructure are optimum.

The presented model of the AMO process in the optimum composition of the electrolyte has been tested experimentally in solving specific problems of increasing the heat resistance of units and mechanisms subjected to heat-cyclic loads.

One example of thermostressed units with the complex configuration of thermostressed surfaces functioning under conditions of heat cycling is the group of pistons in internal combustion engines of highly augmented engines of a new generation where turbosupercharging dictates the necessity of protecting their parts

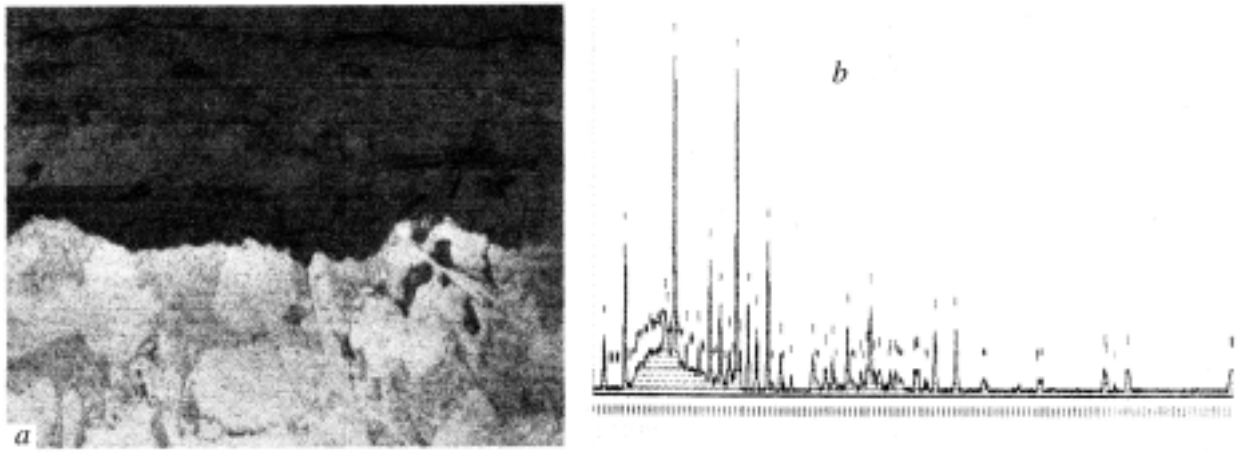

Fig. 6. Structural features of the thermal barrier on the critical piston surfaces: (a) microstructure of the aluminum-based ceramic coating and (b) diffraction pattern from the ceramic-layer surface.

manufactured from casting alloys of aluminum, in particular, of the bottoms and combustion chambers of 245-1004021 pistons against high-temperature heat fluxes going out of the internal combustion chambers.

Formation of ceramic coatings on the bottom and in the combustion chamber of the piston was accomplished in two possible regimes of the AMO process, namely, galvanostatic and potentiostatic. In so doing, we controlled the voltage U, which increased with time as the oxide layer grew, the anodic current I_a, and the coating thickness h. The total time of formation of the coating was 60 min.

The analysis of the experimental data obtained has shown that in the galvanostatic regime of formation of the barrier the voltage exponentially increases with time (Fig. 5a) independently of the initial current density. Moreover, it has been noted that a change in the initial current density does not influence the initial sparking voltage U_s, which in all the experiments was equal to 270 V. However, the duration of the AMO process and the quality of the coatings formed in the indicated regime depend to a great degree on the initial current density. It has been established that for j = 1–2 and 5–6 A/dm^2 it is purposeless to carry out the AMO process. In the first case, this is attributed to the substantial increase in the duration of the process (thus, only attaining the sparking regime takes about 40–45 min) and, moreover, the thickness of the nonuniformly formed coating does not exceed 5 μm, which is confirmed by both the theoretical calculations and the results obtained in practice (Fig. 5b). In the second case, despite the fact that the process quickly reaches the regime of microarc oxidation (in about 10–15 min) (Fig. 5b), the formation of a uniformly thick continuous coating with a thickness of no less than the required 60 μm encounters difficulties due to the intense heating-up of the electrolyte (the temperature attains 85–90^{o}C) and the superhigh intensity of the electric field. This results in the separation of microdischarges to form arcs, which produces the local zones of breakdown and, consequently, degrades the quality of the formed layer and its appearance and decreases the heat-resistance characteristics.

The coatings formed in the indicated regime are, as a rule, highly porous and substantially hydrated and contain in their composition from 10 to 20% of electrolyte anions built-in into the structure of the formed layer independently of the initial microstructure of the casting. In operation of a product treated in such a way, the electrolyte components and water are removed from the oxide layer, thus making it loose and decreasing the properties prescribed [28].

The most acceptable results were obtained for j = 3–4 A/dm^2. Here, reaching the sparking regime took about 25–30 min, and further growth of the coating, as the time of the experiment (60 min) passed, and the microstructure created show the expediency of using this current regime. The high characteristics of con-

TABLE 1. Chemical Composition and Quantitative Characteristics of the Compounds and Elements Contained in the Developed AMO Coating

Chemical compound or element	Composition of the chemical compound or element, %		Chemical compound or element	Composition of the chemical compound or element, %	
	relative	absolute		relative	absolute
Al	20.0	15.5	NaAlSiO	22.1	17.1
CaAlSiO	0	0	SiO_2	12.3	9.6
$MgAl_2O_4$	0.0001	0	Si	0	0
Mullite	36.7	23.6	Al_2O_3	1.0	0.7

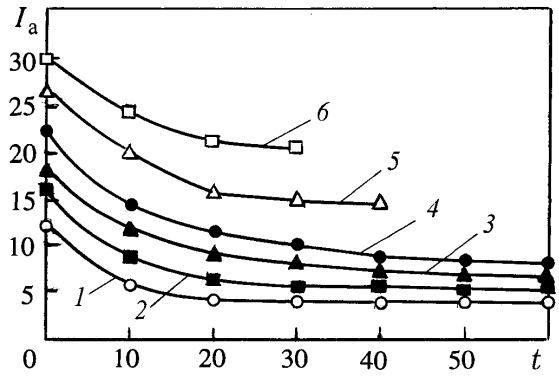

Fig. 7. Change in the anodic current versus time in the potentiostatic regime of the AMO process for the prescribed voltage: 1) U = 210, 2) 240, 3) 370, 4) 300, 5) 330, and 6) 360 V. I_a, A; t, min.

tinuity and density, the monochromaticity of the color range over the entire treated surface without any signs of etching and swelling, and the homogeneous microstructure ensure obtaining stable properties and high adhesion to the base material. The coating thickness was more than 50 μm (Fig. 6a). The phase composition of the coating was similar to the corundum-like ceramics in which, despite the great amount of free silicon, mullite formations and silicon oxides are few, which is evidenced by the absence of a "halo" in the diffraction pattern (Fig. 6b) and by the coating phases presented in Table 1.

In the potentiostatic regime, in which the voltage is prescribed, the kinetics of the process was studied within the range 210–360 V since below 210 V the regime of microarc oxidation was not reached, while for the voltage higher than 360 V microdischarges separated without the AMO stage and formed an arc. Initially, the prescribed voltage changed discretely with a step of 30 V. The anodic current decreased exponentially with time.

For the range 210–270 V, the anodic current abruptly decreased within 5–10 min, after which the current virtually remained unchanged. Reaching the AMO regime took 50 min or more; for this time the electrolyte was heated up to the boiling temperature, which adversely affected the quality of the coatings obtained. For $U > 300$ V, the AMO process was limited by the time interval from 0 to 30 min. As the duration of the process increased, the discharge formed an arc which could result in the formation of burns and the sites of subsequent pitting on the treated surface..

The most reliable results on the quality of the ceramic layer formed were obtained within the voltage range $270 < U < 300$ V (Fig. 7). Here, the AMO coatings on the pistons are characterized by a high level of adhesion to the base; they have a uniform light-gray color, a porosity of about 20%, and a purity of the surface higher than the coatings formed in the galvanostatic regime: AMO $0.3 <$ Ra < 1.6. The thickness of the coatings obtained exceeds 50 μm. The microhardness of the coating is slightly higher than of the galvanostatic coating (1.3–1.8 GPa) and exceeds the microhardness of the base by one order of magnitude.

In comparative tests for heat cycling of the pistons with an AMO coating and without it on a special bench of the Minsk Motor Plant, it has been established that the best pistons of the Machle Company withstood 4000 heat cycles, the pistons without a coating withstood no more than 1800 heat cycles, and the best pistons with an AMO coating withstood 5100 heat cycles [28].

Thus, the investigation carried out and the results obtained have demonstrated good correlation with theoretical calculations and have allowed development of the technology of anodic microarc oxidation and creation of electrolytes whose application to the formation of thermal barriers on complex-configuration critical surfaces of thermostressed units ensures a severalfold increase in their heat resistance under conditions of heat cycling.

NOTATION

U, voltage; I, current; I_i, ionic current; I_a, anodic current; E, field intensity; A and B, empirical constants; dh/dt, rate of change of the thickness of an anodic oxide film; N, number of ions moving through unit cross section normal to the direction of the ionic current; ν, oscillation frequency of ions in the initial position ($\approx 10^{12}$ Hz); q, ionic charge; a_b, half-thickness of the barrier; U_s and $U_{m.d}$, initial voltages; tan β_1, tan β_2, and tan β_3, mean rates of film growth; $j_{1(t)}$, discharge-free, $j_{2(t)}$, spark, and $j_{3(t)}$, microarc transfer of charges; N_2, N_3^*, S_2^*, and S_3^*, numbers of simultaneously burning discharges and areas of their effective cross sections; $j_{2(t)}^*$ and $j_{3(t)}^*$, mean density of the current of a single spark discharge and a single microarc discharge, respectively; T, temperature; k, dielectric constant; t, instant of time; h and m, thickness and mass of the coating, respectively; p^*, mean volume density of the coating layer; U_e, voltage drop in the electrolyte; $a_{i(t)}^*$ and $b_{i(t)}^*$, local parameters; α_1–α_3, coefficients of impact ionization at different instants; β_1, β_2, and β_3, slopes toward the points on the curve which correspond to U_s, $U_{m.d}$, and U_f, respectively; 2θ, angle of deviation of x rays from the surface. Subscripts: s, sparking; f, final; m.d, microarc discharge; a.d, arc discharge; e, electrolyte; i, ionic, a, anodic.

REFERENCES

1. S. Ya. Grilikhes, in: *Oxide and Phosphate Coatings of Metals* [in Russian], Moscow (1985), p. 15.
2. L. L. Ordynets and E. Ya. Khanina, *Physics of Oxide Films* [in Russian], Petrozavodsk (1981).
3. V. I. Chernenko, A. G. Krapivnyi, and L. A. Snezhko, *Properties of Coatings Obtained on Aluminum and Its Alloys from Alkaline Electrolytes in a Spark Discharge* [in Russian], Dep. at UkrNINTI, Kiev (1980), p. 197.
4. É. S. Karakozov, A. V. Chavdarov, and N. V. Barykin, *Svarochn. Proizv.*, No. 6, 53–57 (1993).
5. V. I. Belevantsev, O. P. Terleeva, G. A. Markov, et al., *Zashchita Metallov*, **34**, No. 5, 469–484 (1998).
6. W. McNeil, *J. Electrochem. Soc.*, **105**, No. 9, 544–548 (1958).
7. N. P. Sluginov, *Zh. Rus. Fiz.-Khim. Obshch., Fiz. Chast'*, **10**, No. 8, 241–243 (1878).
8. A. Guntershulze and H. Betz, *Electrolytic Capacitors* [Russian translation], Moscow (1938).
9. A. Girginiv and S. Ikonopisov, *Comp. Rend. Acad. Bulg. Sci.*, **28**, No. 3, 391–393 (1975).
10. A. Guntershulze and H. Betz, *Z. Physik*, **78**, 196–198 (1932).
11. A. V. Timoshenko, B. K. Opara, and A. F. Kovalev, *Zashchita Metallov*, **22**, No. 3, 417–424 (1991).
12. N. M. Chigrinova and V. E. Chigrinov, *Poroshk. Metallurg.*, No. 21, 97–100 (1998).
13. P. S. Gordienko, *Formation of Coatings on Some Metals and Alloys in Electrolytes in Microplasma Processes*, Author's Abstract of Doctoral Dissertation in Technical Sciences, Vladivostok (1991).
14. V. I. Belevantsev, G. A. Markov, O. P. Terleeva, and E. K. Shulepko, *Izv. Sib. Otd. Akad. Nauk SSSR, Ser. Khim. Nauk*, Issue 6, 73–75 (1989).

15. G. A. Markov, V. I. Belevantsev, A. I. Slonova, and O. P. Terleeva, *Élektrokhimiya*, **25**, No. 11, 1473–1476 (1989).
16. M. K. Mironova, *Zashchita Metallov*, **21**, No. 2, 320–323 (1990).
17. G. A. Markov, V. I. Belevantsev, O. P. Terleeva, and E. K. Shulepko, *Trenie Iznos*, **9**, No. 2, 286–290 (1990).
18. A. I. Mamaev, Yu. Yu. Chekanova, and Zh. M. Ramazanova, *Fiz. Khim. Obrab. Mater.*, No. 4, 4–44 (1999).
19. V. I. Chernenko, L. A. Snezhko, and S. V. Chernova, *Zashchita Metallov*, **18**, No. 3, 454–458 (1982).
20. G. A. Markov, O. P. Terleeva, and E. K. Shulepko, *Tr. Mosk. Inst. Neftekhim. Gaz. Prom.* (Moscow), Issue 185, 54–57 (1985).
21. G. A. Markov, O. P. Terleeva, E. K. Shulepko, and V. I. Kirillov, *Formation of Ceramic Coatings by a Microplasmachemical Method*, USSR Inventor's Certificate 1451821, Byul. Izobret., No. 13 (1989).
22. G. A. Markov and E. K. Shulepko, *Élektrokhimiya*, **30**, No. 3, 397–401 (1994).
23. A. V. Timoshenko, I. E. Seregina, A. F. Kovalev, and I. S. Mironov, *Composition and Properties of Anodic Oxide Coatings Formed on V95 Alloy in Different Electrolytes* [in Russian], Moscow (1987).
24. A. P. Efremov and R. L. Bolotov, in: *Ext. Abstr. of Papers Presented at All-Union Meeting in Krasnyi Kurgan* [in Russian], Moscow (1988), p. 22.
25. V. A. Mukhin, V. I. Morozov, Yu. N. Smirnov, and D. I. Kir'yanov, *Distinctive Features of Anodic Films Obtained in Spark-Discharge Mode on Aluminum* [in Russian], Omsk (1983).
26. K.-H. Dittich, W. Krysmann, P. Kurze, and H. Schneider, *Cryst. Res. Techn.*, No. 1, 93–95 (1984).
27. I. Mizuki and N. Baba, *J. Metal Finish. Soc. Jpn.*, **33**, No. 5, 258–262 (1982).
28. N. M. Chigrinova, V. E. Chigrinov, A. A. Kukharev, and V. V. Ovchinnikov, *Litein. Proizv.*, No. 11, 24–26 (1999).